HIGH-FREQUENCY GAS-DISCHARGE BREAKDOWN IN HELIUM

A. D. MacDONALD and SANBORN C. BROWN

TECHNICAL REPORT NO. 86

OCTOBER 23, 1948

RESEARCH LABORATORY OF ELECTRONICS

MASSACHUSETTS INSTITUTE OF TECHNOLOGY

The research reported in this document was made possible through support extended the Massachusetts Institute of Technology, Research Laboratory of Electronics, jointly by the Army Signal Corps, the Navy Department (Office of Naval Research) and the Air Force (Air Materiel Command), under Signal Corps Contract No. W36-039-sc-32037, Project No. 102B; Department of the Army Project No. 3-99-10-022.

MASSACHUSETTS INSTITUTE OF TECHNOLOGY

Research Laboratory of Electronics

Technical Report No. 86 October 23, 1948.

HIGH-FREQUENCY GAS-DISCHARGE BREAKDOWN IN HELIUM

A. D. MacDonald and Sanborn C. Brown

Abstract

Breakdown electric fields in low-pressure helium at high frequencies have been theoretically predicted and experimentally verified. The energy distribution of electrons is derived from the Boltzmann transport equation by taking into account all significant removal processes. The distribution function is expanded in spherical harmonics and the resulting second-order linear differential equation is solved in terms of the confluent hypergeometric function. This distribution function combined with kinetic theory formulas permits calculation of the ionization rate and the electron diffusion coefficient. From these the high-frequency ionization coefficient is determined. Through the diffusion equation this ionization coefficient is related to breakdown electric fields. Thus breakdown electric fields are predicted theoretically without using any gas-discharge data other than experimental values of the excitation potential and collision cross section of helium. Breakdown electric fields are measured for helium in microwave cavities of various sizes with a large range of pressure. The theoretical electric fields, involving no adjustable parameters, are checked within the maximum experimental error of 6 per cent.

HIGH-FREQUENCY GAS-DISCHARGE BREAKDOWN IN HELIUM

Introduction

When a high-frequency electric field is applied to a gas, breakdown occurs when the number of electrons produced by ionization equals the number lost by diffusion.[1] The ionization rate and the diffusion coefficient will be computed theoretically on the basis of kinetic theory. These enable us to predict high-frequency ionization coefficients and breakdown electric fields. The electron distribution function is determined by setting up the electron continuity equation, accounting for production and loss of electrons in phase space. The distribution functions so determined are used in standard kinetic theory formulas in order to find ionization rates and diffusion coefficients. The results are expressed in terms of the high-frequency ionization coefficient ζ [1]

1. Spherical Harmonic Expansion

The phase space continuity equation (Boltzmann transport equation) for electrons may be written as[2,3]

$$P = \frac{\partial f}{\partial t} + \bar{v} \cdot \nabla f + \bar{a} \cdot \nabla_v f, \qquad (1)$$

where f is the electron energy distribution function, P is the production rate of electrons per unit phase space and may be expressed in terms of f by finding the energy changes in electrons for elastic and inelastic collisions; $\bar{v}$ the velocity, $\bar{a}$ the acceleration, t the time, and ∇_v the gradient operator in velocity space.

Collisions with gas atoms tend to disorder any non-random motion of the electrons so that f is almost spherically symmetric. Thus if f is expanded in spherical harmonics $f = f_o + (\bar{v} \cdot \bar{f}_1)/v + \ldots$;[4] the spherically symmetrical term f_o is predominant. The $\bar{f}_1$ term represents a vector drift term from which the current may be calculated. The series then is rapidly convergent and we consider only those cases where the first two terms suffice to calculate the properties of the system.

2. The Differential Equation for f_o

Consider the electric field as sinusoidal in time; on expansion, Eq. (1) becomes[3]

$$P_o = \frac{\partial f_o}{\partial t} + \frac{v}{3u}\frac{\partial}{\partial u}(u\bar{E} \cdot \bar{f}_1) + \frac{v}{3}\nabla \cdot \bar{f}_1 \qquad (2)$$

and

$$\bar{P}_1 = \frac{\partial \bar{f}_1}{\partial t} + v\nabla f_o + v\bar{E}\frac{\partial f_o}{\partial u} \qquad (3)$$

provided P is expanded $P = P_o + (\bar{P}_1 \cdot \bar{v})/v$, and the electric field is represented by $\bar{E}$. An energy variable u is introduced by setting $mv^2/2e = u$, where e is the electronic charge and m is the mass of the electron.

Elastic collisions may be considered as instantaneous processes and the energy loss therefrom may be treated by putting equivalent loss terms $P_{o,el}$ and $\bar{P}_{1,el}$ in the equation. Morse, Allis, and Lamar[3] have shown that

$$P_{o,el} = 2\frac{m}{M}\frac{v}{u}\cdot\frac{d}{du}\left(\frac{u^2 f_o}{\ell}\right) \qquad (4)$$

and

$$\bar{P}_{1,el} = -\frac{v}{\ell}\bar{f}_1, \qquad (5)$$

ℓ being the electronic mean free path, and M the mass of the atom.

In low-pressure helium, recombination is not a significant electron removal process at breakdown. Ionizations and excitations have no angular dependence and therefore make a contribution to P_o only; we represent this contribution due to inelastic collisions by $P_{o,in}$.

The electric field E is represented by $E_o e^{j\omega t}$ where ω is the radian frequency. In the gas, the energy transfer by the field to the electrons depends on E^2 so that the root-mean-square field is all that is required. There follows directly from Margenau's analysis[5] an expression for $\bar{E} : \bar{f}_1$ which is the same as that obtained by considering an effective field E_e defined by

$$E_e^2 = E^2\frac{(v/\ell)^2}{(v/\ell)^2 + \omega^2} \qquad (6)$$

where E is the r.m.s. value of the applied field.

The differential equation for f_o then becomes

$$P_{o,in} + \frac{2m}{M}\frac{v}{u}\frac{d}{du}\left(\frac{u^2 f_o}{\ell}\right) = \frac{\ell v}{3\Lambda^2} f_o - \frac{v}{3u}\frac{d}{du}\left\{\ell u\frac{df_o}{du}\cdot\frac{E^2(v/\ell)^2}{(v/\ell)^2 + \omega^2}\right\}. \qquad (7)$$

Here $\nabla^2 f_o$ has been replaced by $(-1/\Lambda^2)f_o$ by using the diffusion equation.[1] The factor $1/\Lambda^2$ depends on the geometry of the discharge container, and is the

characteristic value in the solution of the diffusion equation; Λ is then the characteristic diffusion length. The mean free path ℓ equals $1/(pP_c)$ if p is the pressure and P_c the probability of collision per cm of path per mm of pressure. There now remains to specify the functional forms of P_c and $P_{o,in}$, to complete the formulation of the equation. Excitation will be effectively eliminated by the introduction of mercury vapor.

3. Expression for the Collision Cross Sections

A good approximation for P_c in helium is $P_c u^{\frac{1}{2}}$ = constant = 43 volts$^{\frac{1}{2}}$/(cm x mm Hg).[6] The experimental curve departs from this form for u less than 4 volts and P_c is roughly constant from u = 0 to u = 4, Most of the collisions the electron makes with gas atoms occur after the electron has an energy of 4 e.v., so that this discrepancy has a small effect on the breakdown field. The solution of the equation will be carried out by assuming $P_c u^{\frac{1}{2}}$ = constant over the whole range of electron energies, and will be corrected in Sec. 5 by finding the distribution function required when this range of constant mean free path is considered.

Helium has a metastable level at 19.8 volts and transitions from this level to the ground state by radiation are forbidden. Since metastable states have mean lives of the order of thousands of microseconds, practically every helium atom which reaches an energy of 19.8 volts will collide with a mercury atom and lose its energy by ionizing the mercury. Therefore each inelastic collision will produce an ionization and the effective ionization potential u_i will be the first helium excitation potential plus a small overshoot energy due to the fact that the most probable energy at excitation is higher than the excitation energy. (The amount of this overshoot is calculated in Sec. 6.) Then $P_{o,in}$ may be assumed zero for $u < u_i$ and infinite for $u > u_i$. Physically this means that there will be no electrons with an energy above that corresponding to $u = u_i$. This condition on the electron population provides a boundary value for the differential equation which we now solve for $u < u_i$, with f_o zero for $u = u_i$.

4. Solution of the Equation and Evaluation of ζ

Equation (7) becomes, on inclusion of results of Sec.3, in the region where $u < u_i$

$$u \frac{d^2 f_o}{du^2} + \frac{df_o}{du}\left[\frac{\mu u}{\beta} + \frac{3}{2}\right] + f_o\left[\frac{3}{2}\frac{\mu}{\beta} - \frac{u}{\beta}\right] = 0 \qquad (8)$$

where

$$\mu = \frac{3m}{M} \frac{m}{e} \frac{\Lambda^2}{\tau^2},$$

and

$$\beta = \frac{1}{\sigma}\left(\frac{E\Lambda}{\omega\tau}\right)^2;$$

τ is the mean free time, $\frac{1}{\tau} = 2.37(10^9)p(\text{in mm Hg})^6$ and

$$\sigma = 1 + \left(\frac{1}{\tau\omega}\right)^2.$$

For convenience we transform to a dimensionless independent variable by letting

$$w = \frac{\mu}{\beta}\sqrt{1 + \frac{4\beta}{\mu^2}}\, u = \frac{\mu b}{\beta} u, \tag{9}$$

and transform the dependent variable by

$$f_o = (g)\exp\left[-\frac{1}{2}\left(\frac{1}{b} + 1\right)w\right]. \tag{10}$$

Then

$$w\frac{d^2g}{dw^2} + \frac{dg}{dw}\left(\frac{3}{2} - w\right) - \alpha g = 0 \tag{11}$$

where

$$\alpha = \frac{3}{4}\left(1 - \frac{1}{b}\right).$$

Equation (11) is the confluent hypergeometric equation[7] and its solutions may be written as[8]

$$g_1 = M\left(\alpha; \frac{3}{2}; w\right) \qquad g_2 = w^{-\frac{1}{2}} M\left(\alpha - \frac{1}{2}; \frac{1}{2}; w\right). \tag{12}$$

For brevity we will use the notation

$$M\left(\alpha; \frac{3}{2}; w\right) = M_1(w) \tag{13}$$

and

$$w^{-\frac{1}{2}}M(\alpha - \tfrac{1}{2};\tfrac{1}{2};w) = M_2(w). \tag{14}$$

Then the distribution function f_o is given by

$$f_o = \left[M_1(w) + CM_2(w)\right] \exp\left[-w(1 - 2/3\ \alpha)\right] \tag{15}$$

where the constant C is determined by the boundary condition that the distribution function go to zero at $u = u_i$; therefore

$$C = -\frac{M_2(w_i)}{M_1(w_i)}.$$

Having determined the distribution function we are in a position to calculate the high-frequency ionization coefficient ζ. By the use of standard kinetic theory formulas and the distribution function expressed in Eq. (15) we calculate the quantities $n\nu$ and nD where n is the electron concentration, ν the ionization rate, and D the diffusion coefficient. The ratio of $n\nu$ to nD divided by the square of the electric field is ζ.

The kinetic theory formula for the number of inelastic collisions per electron per second, ν, is

$$n\nu = -4\pi \frac{2e^2}{m^2} \int_{u_i}^{\infty} \frac{u}{v} P_{o,in}\, du, \tag{16}$$

where $P_{o,in}$ is the production rate of electrons per unit volume of phase space due to inelastic collisions.

The integral in Eq. (16) is an improper integral but $P_{o,in}$ is transformed through Eq. (7) to a function of f_o and u. The resulting rigorous expression is integrated by parts. The integration, subject to the condition that f_o and df_o/du are zero for $u = \infty$, yields

$$n\nu = -\frac{2\pi}{3}\left(\frac{E}{\omega}\right)^2 \frac{1}{\sigma\tau} \left(\frac{2e}{m}\right)^{5/2} \left[u^{3/2} \frac{df_o}{du}\right]_{u = u_i}. \tag{17}$$

Similarly the diffusion coefficient for electrons, D, is

$$nD = \frac{2\pi\Gamma}{3}\left(\frac{2e}{m}\right)^{5/2}\int_0^{u_i} f_o u^{3/2} du \ . \qquad (18)$$

The expression for f_o from Eq. (15) is substituted in the integrand and the integrations performed. The integrals have been evaluated for arbitrary values of the parameters involved.[8]

On carrying out the integrations in Eq. (18), and dividing Eq. (17) by the resulting expression we have the high-frequency ionization coefficient

$$\frac{1}{\zeta} = \frac{DE^2}{\nu} = (E\Lambda)^2\left[M_1(w_i)\exp\left(-\frac{2}{3}\alpha w_i\right) - 1\right] . \qquad (19)$$

The form of Eq. (18) has been simplified by using the fact that the expression

$$M_1'(w_i)M_2(w_i) - M_2'(w_i)M_1(w_i) + \frac{1}{2w_i}M_1(w_i)M_2(w_i)$$

is the Wronskian of the differential Eq. (11) and its value is $\frac{1}{2}w_i^{-3/2}\exp w_i$. At breakdown $\nu/D = 1/\Lambda^2$, so we see from Eq. (19) that the breakdown electric fields may be determined by solving the equation

$$M_1(w_i)\exp\left(-\frac{2}{3}\alpha w_i\right) = 2. \qquad (20)$$

For helium, the numerical values of the variables involved in terms of experimental parameters are

$$w_i = \frac{0.820(10^4)u_i}{(E\lambda)^2}\, b\left[1 + \left(\frac{p\lambda}{79.6}\right)^2\right] \qquad (21)$$

$$b = \left[1 + \frac{(E\lambda)^2}{(p\Lambda)^2}\frac{3.77(10^{-4})}{\left[1 + \left(\frac{p\lambda}{79.6}\right)^2\right]}\right]^{\frac{1}{2}} \qquad (22)$$

$$\alpha = 0.75\,\frac{b-1}{b} \qquad (23)$$

where λ is the free-space wavelength of the electric field in cm, E is the r.m.s. value of the electric field in volts per cm, p is the pressure in mm of Hg and Λ is in cm.

A plot of ζ vs. E/p is given in Fig. 1, computed from Eq. (19). Tables of the functions involved are available.[8] The breakdown electric field may be determined from Fig. 1 by finding the curve through those points where $\zeta = 1/(\Lambda^2 E^2)$.

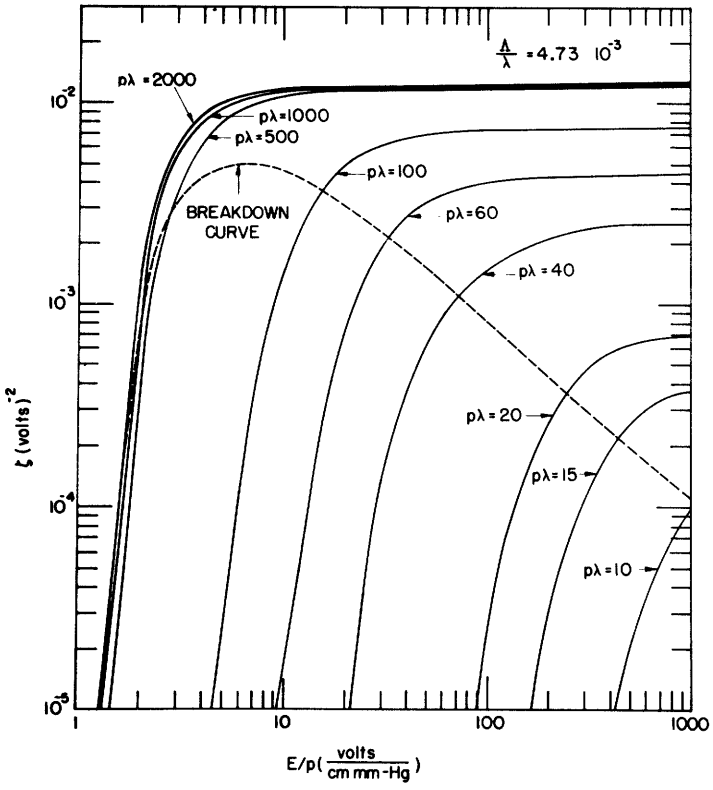

Fig. 1. The high-frequency ionization coefficient ζ computed as a function of E/p from Eq. (19). The breakdown curve is indicated by the dashed line; it is determined by setting $\zeta = 1/(\Lambda^2 E^2)$.

5. Correction for Flat Portion of P_c Curve

From Fig. 2 we see that our approximation for P_c is inaccurate for electron energies below 4 e.v., and therefore in those cases where there are many electrons with low energies, a small correction term may be applied. The low-energy electrons are most important in determining breakdown fields when E/p is small and there are many more collisions per second than oscillations of the field per second, because under these conditions,

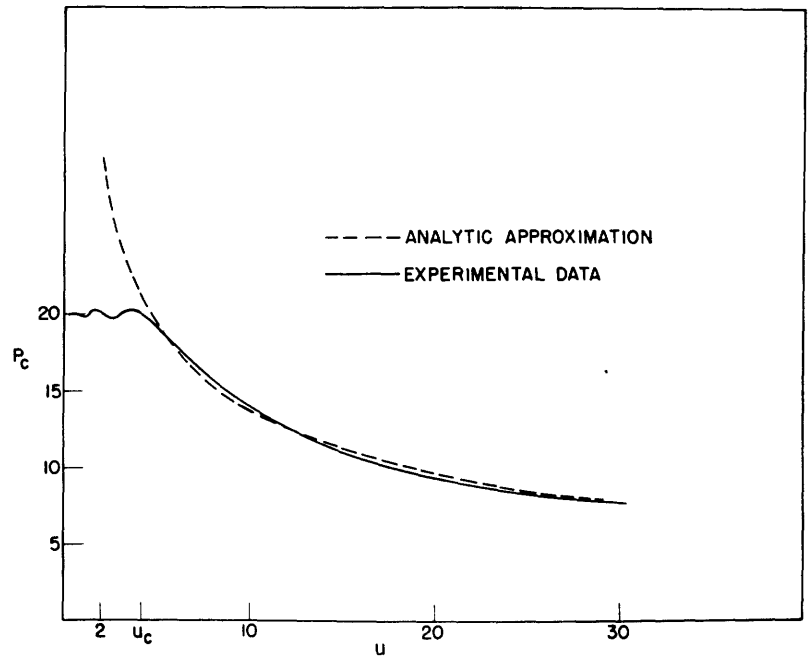

Fig. 2. The probability of collision of electrons in helium at 1 mm of Hg pressure. Brode's experiment is compared with the approximation of this paper.

the relative number of low energy electrons is large. For energies below 4 e.v., Eq. (6) may be simplified by neglecting ω^2 in comparison with $(v/\ell)^2$, and by using the fact that ℓ is constant. The solution may be carried out in the manner of Sec. 4 and f_o is then given by

$$f_o = A\left[M(a;1;y) + BW(a;1;y)\right] \exp(-y) \qquad (24)$$

where M is the confluent hypergeometric function, W is the second solution for integral values of the second parameter,[8,9]

$$a = \frac{1.54}{(p\Lambda)^2},$$

and

$$y = 71.2\left(\frac{p}{E}\right)^2 \left(\frac{u}{u_i}\right)^2,$$

and both functions in Eq. (24) are tabulated.[8]

Again we use a more concise notation for the confluent hypergeometric function by setting

$$M(a;1;y) = M_3(y)$$

and

$$W(a;1;y) = W_3(y).$$

The energy at which P_c changes from a constant to a $u^{-\frac{1}{2}}$ trend is seen from Fig. 2 to be that corresponding to $u_c = u_i/5$. The distribution functions in Eqs. (15) and (24) must be smoothly joined at this energy. By equating the values and slopes of the distribution functions, the constants A and B are determined to be

$$B = \frac{RM_3(y_c) - M_3'(y_c)}{W_3'(y_c) - RW_3(y_c)} \tag{25}$$

where

$$R = \frac{M_1'(w_c) + CM_2'(w_c)\left[1 - \frac{1}{2w_c}\right] + \frac{2}{3}\alpha\left\{M_1(w_c) + CM_2(w_c)\left[1 - \frac{1}{2w_c} + \frac{3}{4\alpha w_c}\right]\right\}}{M_1(w_c) + CM_2(w_c)} \tag{26}$$

and

$$A = \frac{\left[M_1(w_c) + CM_2(w_c)\right]\exp\left[-w_c(1 - \frac{2}{3}\alpha)\right]}{\left[M_3(y_c) + BW_3(y_c)\right]\exp(-y_c)}. \tag{27}$$

This distribution function then modifies the value of the integral for nD and also the expression for ζ in Eq. (19).

The amount of this correction for various cavity sizes and pressures is illustrated in Fig. 3, which shows the correction to be appreciable only for high pressures, and in no case to be more than a few per cent.

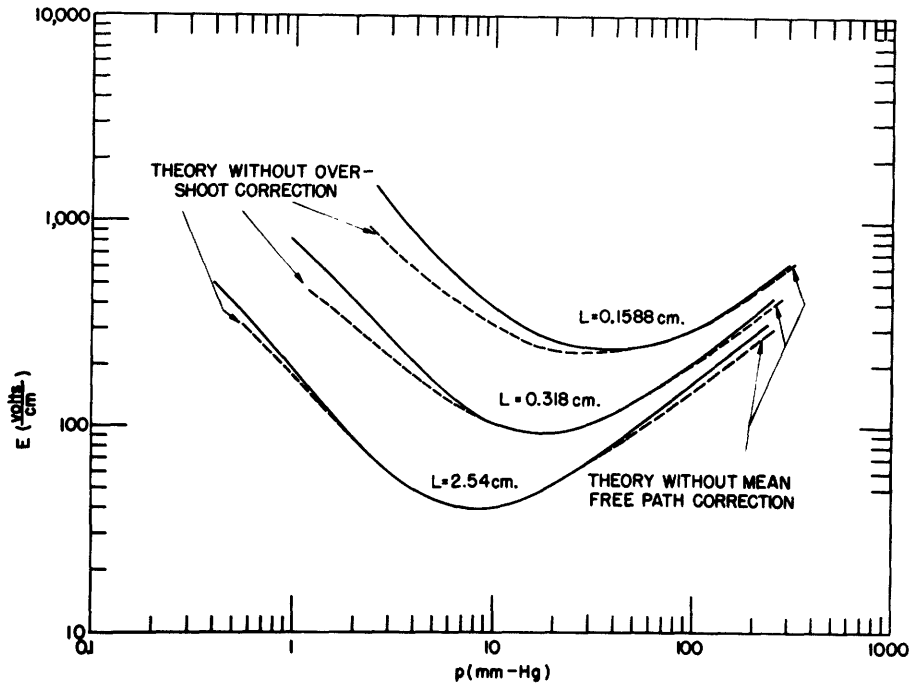

Fig. 3. Theoretical E - p curves illustrating the effect of the correction factors of Secs. 5 and 6. The broken lines indicate theoretical fields without corrections. The 1/8-in. cavity is omitted to avoid confusing the diagram.

6. Correction for Overshoot

The probability of excitation is not infinite at the first excitation potential so that some electrons reach energies above this value before exciting helium atoms. This overshoot in energy is most noticeable at low pressures when the energy gained between collisions is large. To find the energy at which the distribution function goes to zero, we insert the measured values[10] of the excitation function as a loss term in Eq. (8). The excitation function h_x is linear in energy at energies close to the excitation potential. Using Maier-Leibnitz's experimental excitation function[10] for h_x, we may write

$$h_x = \frac{P_x}{P_c} = h_1(w - w_x) = \frac{(u - 19.8)u^{\frac{1}{2}}}{623} \qquad (28)$$

Equation (8) now written in the reduced form and including h_x is

$$\frac{d^2g}{du^2} - Ig = 0 \qquad f_o = (u^{3/4}g)\exp(-\frac{\mu u}{2\beta}) \qquad (29)$$

where

$$I = \frac{1}{\beta}\left[1 + \frac{M}{m}\frac{\mu}{2}h_1 - \frac{1}{u}\left(\frac{M}{m}\frac{\mu}{2}h_1 u_x + 3\mu\right) - \frac{3\beta}{16u^2}\right]. \qquad (30)$$

For $u > u_x$, I may be seen on inspection to be a slowly varying function so that we may solve Eq. (30) approximately and obtain

$$g = \exp(-\sqrt{I}\, u). \qquad (31)$$

Equation (31) combined with Eq. (29) gives the distribution function above the excitation potential; and this distribution function should be fitted to that of Eq. (15). However, the distribtuion function is small in this region and we may determine a voltage at which the distribution function goes to zero by extrapolating Eq. (31) linearly and choosing that voltage where it cuts the axis as the ionization potential. The extrapolation of Eq. (31) yields

$$u_i - u_x = \frac{g}{g'} = \sqrt{I}. \qquad (32)$$

The effective ionization potential is plotted in Fig. 4 for helium as a function of $E\lambda$ with several values of $p\lambda$, for one value of Λ/λ. A more rigorous treatment in which Eq. (29) is solved exactly[8] is possible but does not alter the value of u_i in Fig. 4 significantly.

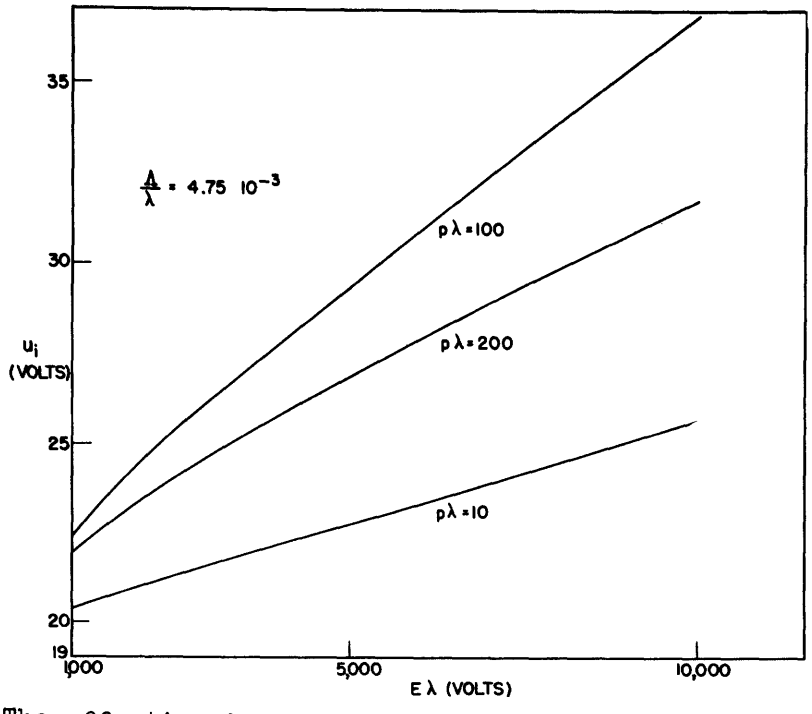

Fig. 4. The effective ionization potential as a function of $E\lambda$ at a constant Λ/λ.

7. Experimental Procedure

A block diagram of the microwave apparatus used in the experiment is shown in Fig. 5. A continuous-wave tunable magnetron in the 10-cm wavelength region supplies up to 150 watts of power into a coaxial line leading to the measuring equipment. A cavity wavemeter receives a small signal from a probe in the line. The power incident on the cavity is varied by a power divider. A directional coupler provides a known fraction of the incident power to a thermistor element whose resistance, measured by a sensitive bridge, indicates power incident on the cavity. A slotted section of line with a movable probe measures the standing-wave ratio and voltage minimum, the probe signal going to a detector with a

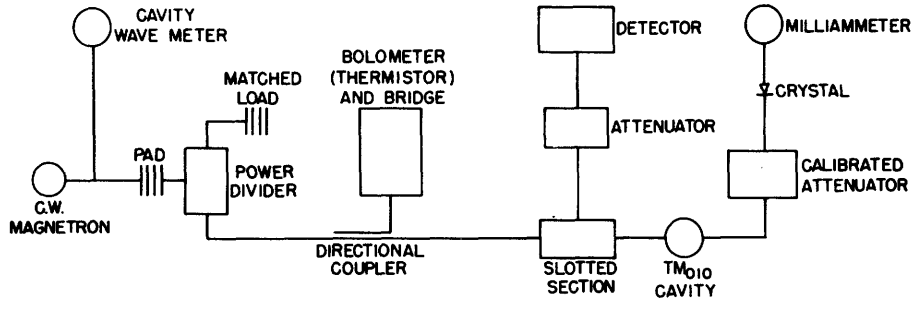

Fig. 5. Block diagram of the experimental microwave equipment.

waveguide-beyond-cut-off attenuator. The cavities resonate in the TM_{010} mode in the 10-cm wavelength region, and are coupled to the coaxial transmission line by a coupling loop. A second coupling loop provides a transmitted signal to an attenuator, crystal, and meter. The electric field is calculated by standard microwave methods.[11,12] The unloaded Q of the cavity is calculated from standing-wave measurements. The power absorbed in the cavity is determined by the measured incident power and the standing-wave ratio. The absorbed power is related to the stored energy through the unloaded Q and the electric field is determined from the known field configuration and the stored energy. It is convenient to calibrate the transmitted signal network in terms of incident power measurements to measure the field.

Care was taken to obtain high gas purity. The cavities were made of oxygen-free high-conductivity copper and all joints were silver soldered. The coupling loops were made of copper, Kovar, and glass. The cavity was connected through Kovar to an all-glass system including a three-stage oil diffusion pump and a liquid-nitrogen trap. Spectroscopically pure helium and distilled mercury were used. Each cavity was baked out for several days at 400°C. and the whole vacuum system carefully outgassed before each run. The mercury pool which introduced the mercury vapor also served to seal the cavity from the liquid air trap during each breakdown field measurement. The

possible effect of direct ionization of mercury in the breakdown process has been investigated theoretically. For the density of mercury used it was found to be not significant in the range of pressures and container sizes used in the experiment.

The breakdown experiment consists of filling the cavity with the gas at a measured pressure, increasing the magnetron power until the crystal current reaches a maximum and drops suddenly to a much lower value. The drop indicates that the gas has broken down and the maximum current indicates the breakdown field. The electrons required to initiate the discharge are provided by a radioactive source near the cavity. The breakdown measurements were reproducible within an experimental error of less than 5 per cent in electric field and less than 1 per cent in pressure. Experiments were done on four cylindrical cavities having a diameter of 8.140 cm and heights of 0.1588, 0.3175, 0.4760, and 2.540 cm. The cavity whose height was great enough so that it could not be considered a parallel-plate system was computed using a non-uniform field theory.[13]

Figure 6 presents the experimental and theoretical E vs. p curves. In Fig. 7 ζ vs. E/p curves computed from the experimental data are compared with theory.

8. Conclusions

The high-frequency ionization coefficient has been calculated theoretically on the basis of the electron continuity equation by considering diffusion to the container walls as the only removal process. It is expressed in terms of $E\Lambda$, $p\lambda$, and $p\Lambda$. The high-frequency ionization coefficient has been derived theoretically in Eq. (19). The ionization coefficient had been previously related to breakdown fields through the diffusion equation.[1]

Equation (20), containing no adjustable gas-discharge data or constants, and involving only the excitation potential and collision cross section of helium, enables us to predict breakdown electric fields. It has been derived from the electron velocity distribution function given by kinetic theory, and the diffusion equation. The agreement between theory and experiment over a wide range of pressure and container-size variation verifies the correctness of the approach.

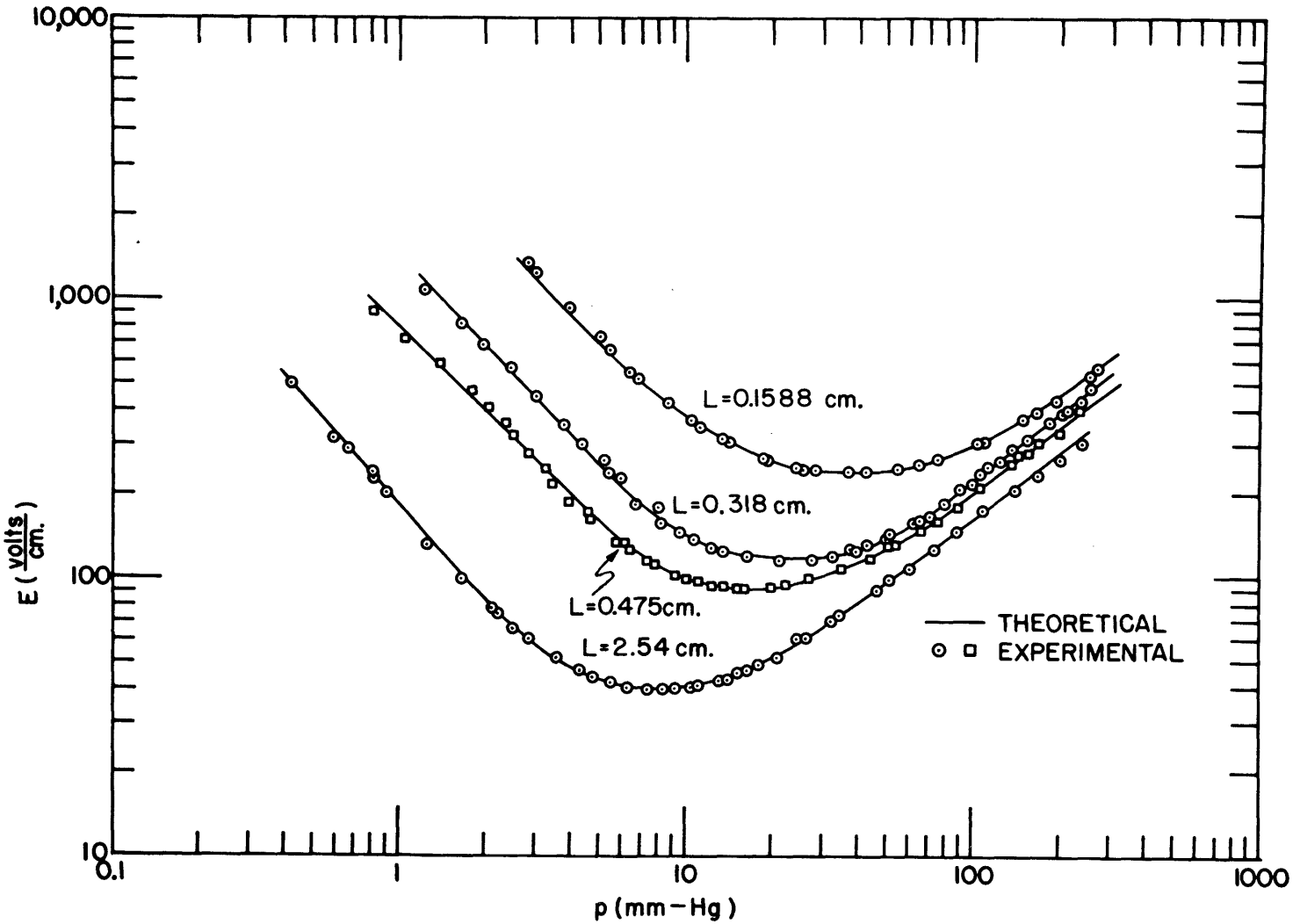

Fig. 6. Experimental breakdown electric fields compared with those theoretically predicted.

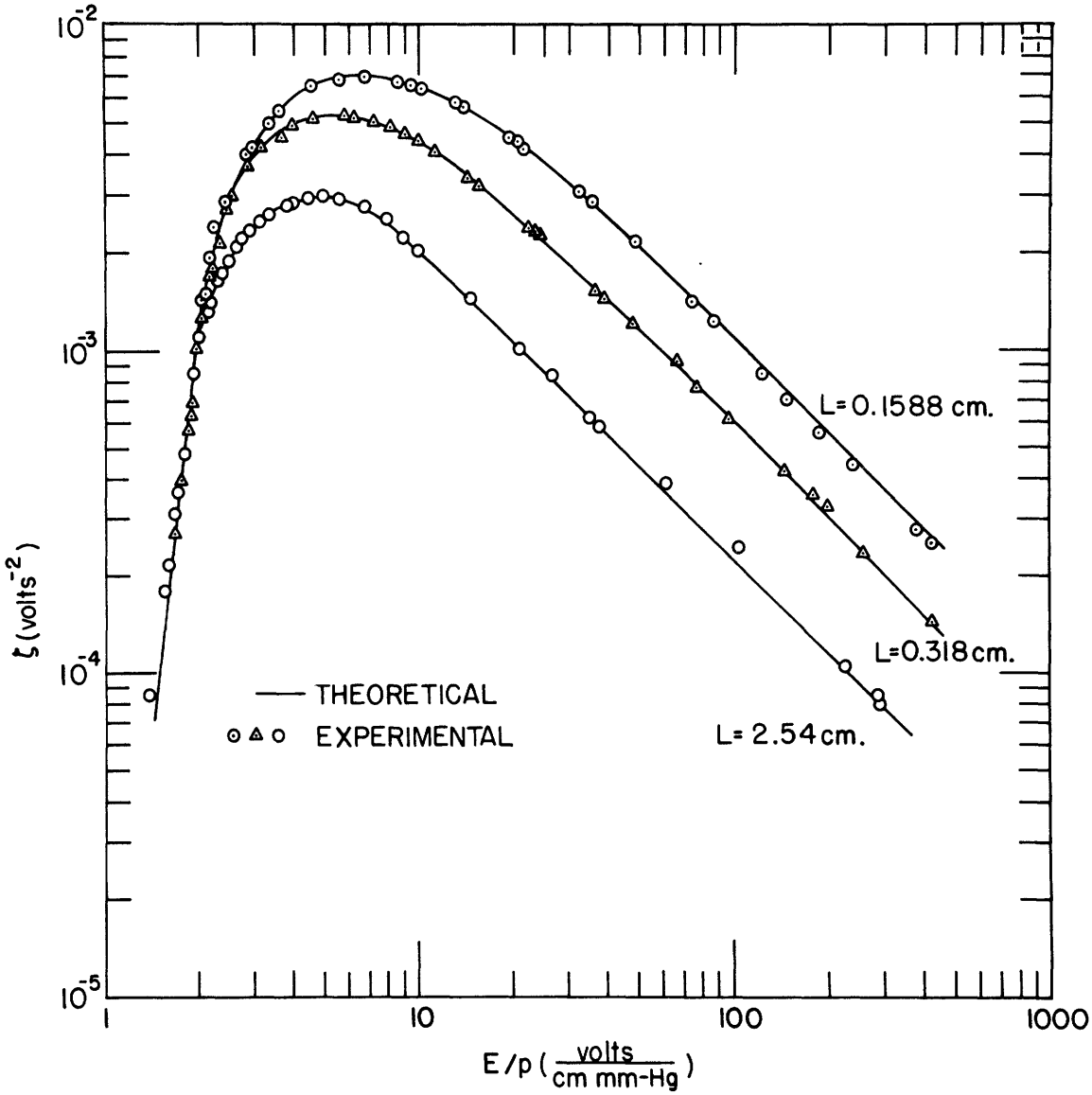

Fig. 7. Experimental ionization coefficient compared with theoretically predicted coefficients. The 1/8-in. cavity is omitted to avoid confusing the diagrams.

Acknowledgment

The authors wish to acknowledge the many valuable ideas contributed by Professor W. P. Allis in numerous discussions leading to the solution of this problem.

References

1. M. A. Herlin and S. C. Brown, RLE Technical Report No. 60, Phys. Rev. 74, 291 (1948).
2. S. Chapman and T. G. Cowling, "The Mathematical Theory of Non-Uniform Gases", Cambridge University Press, Ch. 3 (1939).
3. P. M. Morse, W. P. Allis, and E. S. Lamar, Phys. Rev. 48, 412 (1935).
4. H. Margenau, Phys. Rev. 73, 303 (1948) Eq. (26).
5. H. Margenau, Phys. Rev. 73, 303 (1948) Eq. (27).
6. R. B. Brode, Rev. Mod. Phys. 5, 257 (1933).
7. E. Jahnke and F. Emde, "Funktionen Tafeln", 275, Teubner, Leipzig (1933).
8. A. D. MacDonald, "Properties of the Confluent Hypergeometric Function", Technical Report No. 84, Research Laboratory of Electronics, M.I.T.
9. W . J. Archibald, Phil. Mag., 7, 26, 419 (1938).
10. H. Maier-Leibnitz, Zeit. f. Physik, 95, 499 (1935).
11. C. G. Montgomery, "Microwave Techniques" McGraw-Hill, New York (1947).
12. S. C. Brown et al, "Methods of Measuring the Properties of Ionized Gases at Microwave Frequencies", RLE Technical Report No. 66, May 17, 1948.
13. M. A. Herlin and S. C. Brown, Phys. Rev. 74, 910 (1948).